Automatic Generation of Synthetic Retinal Fundus Images

Samuele Fiorini[12]
samuele.fiorini@studenti.unipd.it
Lucia Ballerini[2]
luciaballerini@computing.dundee.ac.uk
Emanuele Trucco[2]
manueltrucco@computing.dundee.ac.uk
Alfredo Ruggeri[1]
alfredo.ruggeri@unipd.it

[1] Department of Information Engineering
University of Padova
Padova, ITALY

[2] VAMPIRE project, CVIP group
School of Computing
University of Dundee
Dundee, UK

Abstract

This study aims to generate *synthetic* and *realistic* retinal fundus colour images, similar in characteristics to a given dataset, as well as the values of all morphological parameters. A representative task could be, for example, the synthesis of a retinal image with the corresponding vessel tree and optic nerve head binary map, measurement of vessel width in any position, fovea localisation and so on. The presented paper mainly focuses on the generation of non-vascular regions (i.e. retinal background, fovea and optic disc) and it is complemented by a parallel study on the generation of structure and texture of the vessel network. To synthesise convincing retinal backgrounds and foveae, a *patch-based* algorithm has been developed; *model-based* texture synthesis techniques have also been implemented for the generation of realistic optic discs. The validity of our synthetic retinal images has been demonstrated by *visual inspection* and *quantitative experiments*.

1 Introduction

Retinal fundus imaging is a very helpful tool for the diagnosis of many diseases such as diabetes, glaucoma and cardiovascular conditions [1]. This is reflected by the large number of algorithms for optic disc (OD) detection, vessel segmentation and width measurements [8]. In order to evaluate performance, limitations and clinical applicability of a medical image analysis algorithm, a validation step is mandatory. Validation can be defined as *the process of showing that an algorithm performs correctly by comparing its output with a reference standard* [11]. Algorithm validation on manually annotated ground truth (GT) images is a well documented and necessary practice. However, it is also well known that obtaining large quantities of annotated medical GT images is an expensive and laborious task.

The main purpose of this work is the generation of synthetic high resolution retinal fundus images (Figure 1a) in a controlled manner along with a synthetic GT free from inter-observer variability. In the synthesised retinal phantoms, textural anatomical features can be modified to simulate a wide range of parameters and different populations. Our synthetic data would allow extensive validation of algorithms for segmentation and analysis of

anatomical structures. The final goal is the public release of a new database containing synthetic retinal images including OD and macula centre coordinates, vessel binary maps and width at any position and artery/vein classification. All these measurements are of crucial importance during the validation of retinal image analysis algorithms. Medical phantom images are extensively used in many medical imaging environment, but, to our best knowledge, no previous work on the automatic generation of retinal phantoms has ever been proposed.

This initial project has been based on the publicly available *High-Resolution Fundus* (HRF[1]) *Image Database* [7], which has 45 high-quality images at the resolution of 3504×2336 pixels. The generated retinal phantoms have the same size, but images of every resolution can be synthesised by the presented method, given an appropriate dataset.

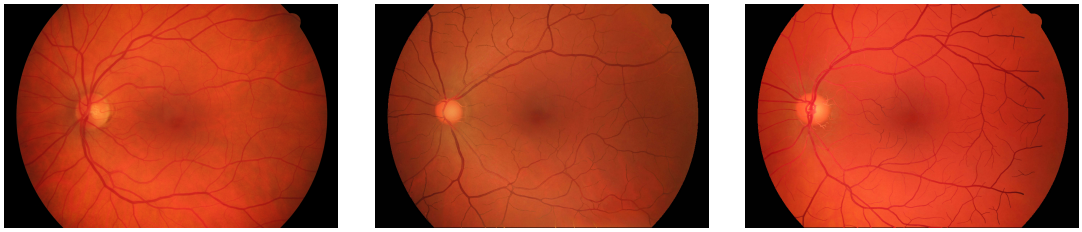

(a) (b) (c)

Figure 1: A comparison between a real retinal fundus image from the HRF dataset (a) and two synthetic phantoms generated with our method (b) and (c).

This paper is organised as follows, in Section 2 we describe the proposed method providing details for both the patch-based (Subsection 2.2) and the model-based (Subsection 2.3) texture synthesis algorithm we propose for the generation of background, fovea and OD. Section 3 describes the conducted experiments and the achieved results. Finally in Section 4 we present our conclusions and some hints for future works.

2 Method

2.1 Overview

In order to generate convincing retinal fundus image phantoms, we started from the observation of real images. At a first glance, retinal images are showing three obvious elements surrounded by an orange-red background: Optic Disc, Vessel Network and Fovea. The background presents a variety of textures. Brightness is also non-uniform across the image, usually brighter in vascular regions and darker in the fovea and in the image periphery. Intuitively the average colour distribution in retinal images could remind us of a *horseshoe* (see Figure 2). Choroidal vessels are also sometimes visible in transparency, this effect creates a real texture, very different from a mere smooth colour fill. In order to synthesise a new background preserving both non-uniform colour distribution and texture characteristics, we developed a patch-based tiling algorithm inspired by Efros and Freeman's *Image Quilting* technique [3], where novel images are synthesised by stitching together small examples of existing images. On the other hand, for the generation of synthetic ODs a novel model-based approach has been followed. This method relies on the idea of learning the distributions of key morphometric quantities from real images and realistically reproduce them.

[1]The HRF database can be downloaded at http://www5.cs.fau.de/research/data/fundus-images/

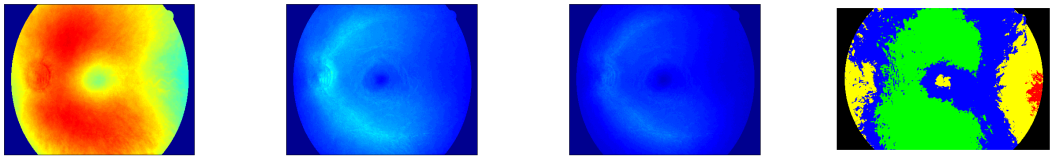

(a) (b) (c) (d)

Figure 2: An example of colour intensity distribution map (CM) in red (a), green (b) and blue (c) channels and the correspondent clustering map (c-CM) (d).

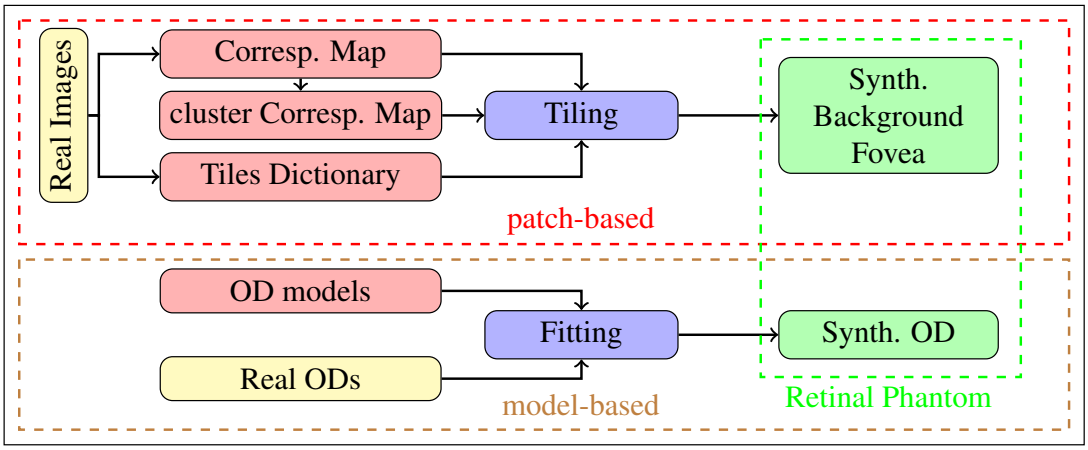

Figure 3: Block diagram depicting the overall method to generate synthetic retinal images.

2.2 Background and Fovea generation

In this section we will discuss about the generation of background and fovea achieved by the previously described patch-based algorithm. As we can see (Figure 3) the tiling algorithm needs three inputs: *a*) a Correspondence Map (CM); *b*) a consistent cluster-CM (c-CM) and *c*) a suitable Tiles Dictionary (TD). For our purposes, a CM is a spatial map of the corresponding colour intensity distribution over the real and the synthetic images. The CM allows our tiling algorithm to recreate a realistic background texture. Different CMs have been created by weighted averaging of 15 real preprocessed images (the healthy HRF subset). The preprocessing consisted in a naive co-registration step followed by a more sophisticated foreground (OD and vessel tree) inpainting. The co-registration step consists in a rigid rotation and a translation of all the images in order to make them share a common polar coordinate system centred on the OD. For the foreground inpainting step we took advantage of the technique proposed by Criminisi *et al*. in [2]. An example of CM is shown in Figure 2.

The tiling algorithm can generate realistic backgrounds and foveae stitching together blocks (tiles) collected from real images. For the generation of our retinal phantoms we collected more than $300,000$ vessel-free tiles 7×7 pixels and we organised them in a TD. To facilitate the research of matching blocks performed by the proposed tiling algorithm, all the collected vessel-free tiles have been grouped into clusters using a pixel-wise K-means algorithm. The number of clusters (4) has been optimised using the Akaike Information Criterion [6] and the feature selected for the clustering were the red and green intensity value of each pixel. Each tile has then been assigned to a unique cluster by means of majority vote. To link this idea with the CM, a consistent c-CM, which shows the distribution of clusters in the CM, has been evaluated as well.

For the description of the proposed tiling algorithm a syntax consistent with [3] has been chosen. To assess the colour similarity among the tiles, the original *error surface* e has been replaced with a *new error surface* ε defined in Equation 1 (where the symbol $\circ$ indicates the element-wise matrix product and the two indexes $n_{<C_1,C_2>}$ and $\gamma_{<C_1,C_2>}$ are, respectively, the grey level and the chroma similarity indexes described in [5]).

$$\varepsilon_{<C_1,C_2>} = 1 - n_{<C_1,C_2>} \circ \gamma_{<C_1,C_2>} \tag{1}$$

The tiling algorithm workflow can be described as follows. Let Φ be the desired output image and $\tau_k(i)$ the *i-th* element of the TD assigned to the cluster ω_k. The final result can be achieved going trough Φ in raster scan order in steps of the size of the tiles minus an overlap (3 pixels) and iterating the following steps:

1. Randomly pick up successive $\tau_k(i)$ from ω_k (where k is defined by the c-CM) until the best match, defined as the tile that locally satisfies the two constraints below, is found:
   - local consistence with the CM: the Euclidean distance between the picked-up tile and the correspondent tile in the CM is less than a threshold T_1;
   - local consistence among the neighbouring blocks in the overlap areas: more than the 90% of the pixels values of the evaluated error surface ε must be less than a threshold T_2.
2. Compute the Cumulative Minimum Error between the overlapping areas defined as $E_{i,j} = \varepsilon_{i,j} + min(E_{i-1,j-1}, E_{i-1,j}, E_{i-1,j+1})$ where $i = 2,\ldots,N$ $j = 2,\ldots,M$ and ε is $N \times M$.
3. Finally, place the new tile cutting out its edges as delineated by a Best Boundary Cut (i.e. the minimum value in each row/column of E) and repeat.

The two thresholds (T_1 and T_2) have been heuristically determined (10 and 0.05 respectively), as well as the default tiles and overlap dimension.

2.3 Optic Disc generation

The OD appears usually as a slightly irregular ellipse with a small inner depression, called cup. The edge of the OD is more evident in the red channel, while the inner cup is usually best highlighted in the green and blue ones. Therefore, to reproduce the same visual effect, we developed two parametric intensity models, one for the red (Equation 2) and one for both the green and the blue channels (Equation 3, where the meaning of the two parameter vectors $\bar{p} = [x_0, y_0, z_0, a, \sigma_1, A, \omega]$ and $\bar{q} = [\bar{p}, x_0, y_0, \sigma_2, k]$ will be clarified below):

$$f_R(x,y,\bar{p}) = z_0 - \frac{1}{a + \exp\left[-\left(\frac{x-x_0+A\cos(\omega t)}{\sigma_1}\right)^2 - \left(\frac{y-y_0+A\cos(\omega t)}{\sigma_1}\right)^2\right]} \tag{2}$$

$$f_{GB}(x,y,\bar{q}) = f_R(x,y,\bar{p}) + k\exp\left[-\left(\frac{x-x_0}{\sigma_2}\right)^2 - \left(\frac{y-y_0}{\sigma_2}\right)^2\right] \tag{3}$$

The two models refer to a three-dimensional space, where the horizontal plane (x,y) is the image plane and the vertical axis z is the colour intensity expressed in the (r,g,b) colour

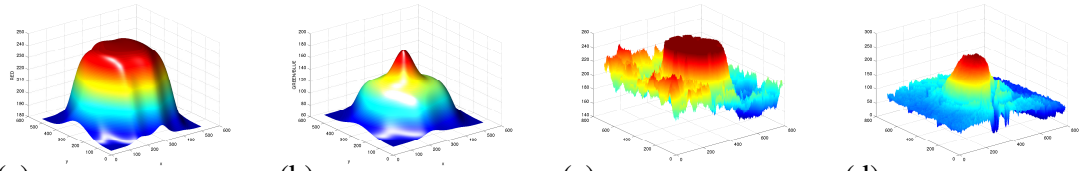

(a) (b) (c) (d)

Figure 4: OD intensity models on the red (a), the green and the blue (b) channels. Real OD data on the red (c) and green (d) channels.

space. The OD generation workflow is described in the lower section of Figure 3. The parameters of the models have been estimated over 30 HRF images (15 healthy and 15 diabetic retinopathy) using a weighted nonlinear least squares criterion. Looking at Figure 4 an explanation of the meaning of the parameters could be provided as follows. While (x_0, y_0, z_0) simply control the translation of the surface along the axes, σ_1 controls the spread of the surface in the horizontal plane (similarly to the standard deviation in the Gaussian component, σ_2). Tuning a we can also modulate the amplitude of the surface. Figure 4a has a low frequency oscillating sinusoidal term that models the irregularity on the OD edges (the cosine in Equation 2 is evaluated in $[0, \cdots, 2\pi]$). Equation 3 presents a symmetrical Gaussian surface that models the inner cup pallor. A suitable probability distribution has been evaluated for each parameter. Convincing ODs can be then synthesised by random sampling a set of parameters from the relative estimated distribution and then evaluating with them Equation 2 and 3.

3 Results

This paper focuses on the generation of non-vascular regions; our preliminary retinal phantoms present synthetic backgrounds and ODs, but vessel networks collected from real healthy HRF images using the provided manually segmented vessel map. Figure 1 shows a comparison between a real retinal fundus image (a) and two examples from our synthetic phantoms databases (b,c). The first results look promising: the generated retinal backgrounds seem to reproduce a realistic colour intensity distribution and a realistic representation of the fovea has been achieved as well. The synthetic ODs look also realistic, they show a natural colour intensity with a correctly placed inner cup and their edge looks realistically merged with the surrounding background.

The main intended purpose of our synthetic image generator is to provide a dataset along with GT images (all parameters known) to validate retinal image analysis algorithms. Assuming that the images are affected by additive Gaussian noise, we compared the estimation of the noise variance σ^2 (evaluated as suggested in [4]) between 15 real HRF and 15 synthetic images. The obtained values are $\sigma^2_{real} = 0.020$ and $\sigma^2_{synth} = 0.022$. Then, we validated our results proving that in the non-vascular regions no vessel-like patterns are created by our method. No intensity adjustment has been provided for the vessel network, so the considered test only concerns the false positive values. We used the well-known algorithm by Soares *et al*. [9] to detect vasculature maps on 15 retinal phantoms and on 15 healthy HRF images provided with manual GT; then we compared the two obtained false positive rate ($FPR = \frac{FP}{FP+TN}$). Using a two-sample Komolgorov-Smirnov test no significant difference at the 5% level can be observed between the FPR obtained from the vessel detection on the two datasets. The average FPR is 0.0097 ad 0.0112 on real and on synthetic images, respectively.

4 Conclusions

In this paper a novel technique for the automatic generation of synthetic retinal fundus images has been presented. A realistic representation of the non-vascular regions (background, fovea and OD) has been achieved and we are currently working on the generation of structure and texture of synthetic vessel trees as well as retinal abnormalities. To our best knowledge, no similar method has been reported in literature. The validity of our retinal phantoms has been supported by visual inspection and quantitative experiments. We are aware of the preliminary nature of the conducted test and we plan a more complete analysis with automatic estimates of further parameters using VAMPIRE [10] and subjective evaluations by clinicians. However, the presented results let us sense that we are correctly moving towards the generation of a synthetic dataset for the validation of retinal image analysis algorithms.

Acknoledgements: Research partially supported by Leverhume trust grant RPG-419. We thank Roberto Annunziata and Enrico Pellegrini for valuable comments and inspiring ideas.

References

[1] M. D. Abràmoff, M. K. Garvin, and M. Sonka. Retinal imaging and image analysis. *IEEE T-MI*, 3:169–208, 2010.

[2] A. Criminisi, P. Pérez, and K. Toyama. Region filling and object removal by exemplar-based image inpainting. *IEEE Trans. on Image Processing*, 13(9):1200–1212, 2004.

[3] A. A. Efros and W. T. Freeman. Image quilting for texture synthesis and transfer. In *Proc. of SIGGRAPH'01*, pages 341–346. ACM, 2001.

[4] D. Garcia. Robust smoothing of gridded data in one and higher dimensions with missing values. *Computational Statistics & Data Analysis*, 54(4):1167–1178, 2010.

[5] P. Guobing, X. Fang, and C. Jiaoliao. A novel algorithm for color similarity measurement and the application for bleeding detection in WCE. *IJIGSP*, 3(5):1, 2011.

[6] C. D. Manning, P. Raghavan, and H. Schütze. *Introduction to information retrieval*, volume 1. Cambridge university press Cambridge, 2008.

[7] J. Odstrcilik, R. Kolar, A. Budai, et al. Retinal vessel segmentation by improved matched filtering: evaluation on a new high-resolution fundus image database. *IET Image Processing*, 7(4):373–383, 2013.

[8] N. Patton, T. M. Aslam, T. MacGillivray, et al. Retinal image analysis: concepts, applications and potential. *Progress in retinal and eye research*, 25(1):99–127, 2006.

[9] J.V.B. Soares, J.J.G. Leandro, R.M. Cesar, et al. Retinal vessel segmentation using the 2-D Gabor wavelet and supervised classification. *IEEE T-MI*, 25(9):1214–1222, 2006.

[10] E. Trucco, L. Ballerini, D. Relan, et al. Novel VAMPIRE algorithms for quantitative analysis of the retinal vasculature. In *Proc. IEEE ISSNIP/BRC*, pages 1–4, 2013.

[11] E. Trucco, A. Ruggeri, T. Karnowski, et al. Validating retinal fundus image analysis algorithms: Issues and a proposal. *Investigative Ophthalmology & Visual Science*, 54 (5):3546–3559, 2013.